Quantitative considerations of dissolved barium as a tracer in the Arctic Ocean

John Ryan Taylor[1] and Kelly Kenison Falkner

College of Oceanic and Atmospheric Sciences, Oregon State University, Corvallis, Oregon, USA

Ursula Schauer

Alfred Wegener Institute for Polar and Marine Research, Bremerhaven, Germany

Mike Meredith

Bidston Observatory, Proudman Oceanographic Laboratories, Prenton, UK

[1] Dissolved barium (Ba) was measured along transects across Fram and Denmark Straits as part of the 1998 ARK-XIV/2 *Polarstern* expedition. Results are combined with other available tracer observations to analyze water mass composition at Fram Strait. A combination of Pacific water and Eurasian river runoff dominated (>80% and >10% of the total mass, respectively) the upper East Greenland Current (EGC), while the remainder of the section was dominated by North Atlantic water. A much smaller contribution of Pacific water to the EGC ($\approx$50%) at Fram Strait in 1987 suggests that this component can be quite variable in time. North American river water was not detectable at Fram Strait in 1998. Presumably, the Eurasian river water we observed at Fram Strait transited eastward along shelf within the Arctic, mixed with Pacific water in the vicinity of the East Siberian Sea, and was borne by the transpolar drift across the Arctic Ocean. In the absence of significant net ice formation along the way such a pathway can be expected to produce more pronounced freshening of the EGC than when Eurasian river water mixes more directly off shelf into salty Atlantic waters and Pacific water is diverted largely through the Canadian archipelago. Existing measurements at the main Arctic gateways were used to construct a Ba budget for the Arctic Ocean under conditions of simultaneous mass, heat, and salt conservation. This preliminary budget is statistically consistent with the steady state hypothesis. On the Arctic basin scale, Ba appears to be conservative. *INDEX TERMS:* 4207 Oceanography: General: Arctic and Antarctic oceanography; 4808 Oceanography: Biological and Chemical: Chemical tracers; 4283 Oceanography: General: Water masses; 4271 Oceanography: General: Physical and chemical properties of seawater; *KEYWORDS:* Arctic Ocean, barium, tracers

1. Introduction

[2] Since it was first postulated that dissolved barium (Ba) might prove to be a useful tracer in upper Arctic Ocean waters [*Falkner et al.*, 1994], over 10,000 Arctic seawater, river, and ice samples have been analyzed in our laboratory. The data cover much of the geographic extent of the region and include at least one sampling of the major gateways of the Arctic at Fram Strait (this study), Barents Sea (K. Falkner, unpublished data, 1997), Bering Strait [*Falkner et al.*, 1994], the Canadian archipelago passages (Falkner et al., Findings from an August 1997 tracer hydrographic survey in passages of the Canadian archipelago, Hudson Strait, and Davis Strait, manuscript in preparation, 2003, hereinafter referred to as Falkner et al., manuscript in preparation, 2003), and the major rivers [*Guay and Falkner*, 1998]. From initial results, we have learned that Ba is highly enriched in North American rivers with respect to Eurasian rivers and typical surface seawater [*Guay and Falkner*, 1998].

[3] Barium is also enriched with respect to underlying waters in the upper halocline layer (salinity $\approx$ 33.1) that originate at Bering Strait [*Guay and Falkner*, 1997] and carries a distinctive siliceous acid ([H_2SiO_3], more simply expressed as Si) maximum [*Jones and Anderson*, 1986]. Elevated Ba contents in surface and subsurface waters occur throughout the Beaufort Gyre, marking the influence of the Mackenzie River and Bering Strait inputs, respectively [*Guay and Falkner*, 1997; *Macdonald et al.*, 1999]. While Eurasian rivers are not as enriched as the Mackenzie, their Ba contents do exceed that of background Atlantic seawater

---

[1]Now at Department of Mechanical and Aerospace Engineering, University of California, San Diego, La Jolla, California, USA.

into which they flow. This contrast has been applied to tracking river water pathways within the Laptev Sea, where the regional prevailing summer wind direction appears to dictate whether river waters are carried across versus along the shelf [*Guay et al.*, 2001].

[4] Findings to date have been based largely on qualitative examination of the Ba distributions. This study explores the foundations of more quantitative treatments of this tracer for Arctic circulation studies. First, Ba sections from Fram Strait and south along the Greenland coast in the vicinity of Denmark Strait are presented. An approach for combining Ba with other tracers to map water mass contributions across these sections is then developed. Fluxes of Ba both into and out of the Arctic at Fram Strait are estimated from this data. Together with existing flux estimates into the Arctic from rivers and Bering Strait and out of the Arctic through passages of the Canadian archipelago, the results are used to generate a first-order budget for Ba in the Arctic. To determine whether the Ba budget can be considered to be at steady state, we take an inverse approach [*Goldner*, 1999], conserving mass, heat, salt, and Ba. The quantitative bounds and uncertainty estimates for the boundary fluxes provided by this exercise are essential prerequisites for exploiting Ba as a tracer in inverse or numerical models for the Arctic.

2. Observations

2.1. Methods

[5] Seawater samples for Ba analyses were obtained during the ARK-XIV/2 expedition of the R/V *Polarstern* that took place from 27 August to 15 October 1998 [*Fahrbach*, 1999]. While the cruise consisted of 282 hydrographic stations comprising multiple sections, Ba was sampled in detail only on section 3 at Fram Strait and sections 7 and 8 in the vicinity of Denmark Strait (Figure 1). Note that section 3 is the only location for which a full set of oxygen isotope measurements is also available. Water samples were obtained using a 24-position rosette comprising 12-L Ocean Test Equipment bottles, an SBE911+ conductivity-temperature-depth sensor, and an RDI 150-kHz narrowband acoustic Doppler current profiler. Samples were collected into 20-mL polyethylene vials that had been precleaned by soaking in 0.2 N HCl overnight at 60°C, followed by copious rinsing with reverse osmosis deionized water and drying in a laminar flow bench. Samples were stored at room temperature and shipped by air back to our laboratory for analysis within a year of collection.

[6] Isotope dilution Ba measurements were conducted on our Excel Plasmaquad inductively coupled plasma quadrupole mass spectrometer (ICPMS) using a procedure similar to one described previously [*Guay*, 1997]. Aliquots (250 μL) of the sample were spiked with an equal volume of a ^{135}Ba-enriched solution (Oak Ridge National Laboratories) diluted twentyfold with 0.2 N HCl and vortex-mixed in a polypropylene test tube. Samples were introduced via a peristaltic pump ($\approx$1 mL min^{-1}) coupled to a Meinhard concentric nebulizer and a cyclone spray chamber. The ICPMS was operated in a peak jump mode, and data were accumulated in three 20-s intervals for masses 135 and 138. A 4-min washout with 0.2 N HCl
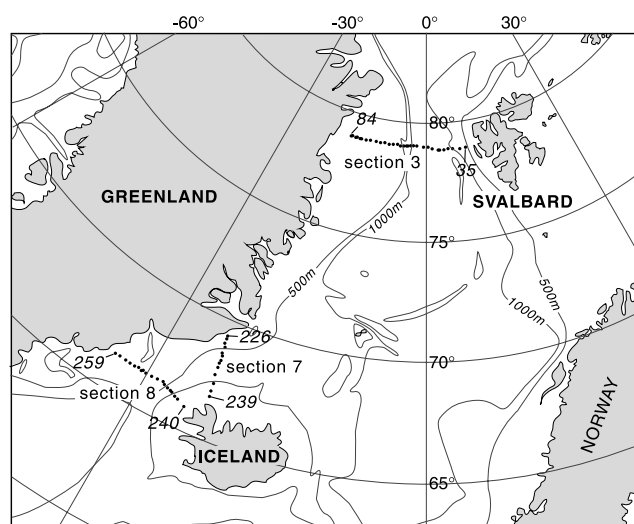

Figure 1. Station locations for Ba sampling on the August–October 1998 ARK-XIV/2 *Polarstern* expedition. Section 3 (east to west stations 35, 40–42, 44–46, 49, 50, 62–64, 66–84) spans Fram Strait. Sections 7 (north to south stations 226–239, excluding 230) and 8 (east to west stations 240–259, excluding 243) are located near Denmark Strait. No Ba data are available for the western half of section 8. Smoothed bathymetric contours at 500 and 1000 m were derived from the General Bathymetric Chart of the Oceans (GEBCO) database.

was performed to diminish memory effects. A blank and a monitor consisting of a spiked Ba standard solution bracketed every five samples. The monitor was used to correct for mass bias. In addition, a consistency standard derived from a large volume of well-characterized seawater and random repeats of two samples were included with each tray (44 positions) of the autosampler. The consistency standard provides a run-to-run check on the spike solution. On the basis of repeated runs of the consistency standard and sample repeats the 2-sigma precision of the analysis ranges from 4% at 10 n*M* to 2% or better at $\geq$50 n*M*. To avoid uncertainties associated with the stoichiometry of BaCO$_3$ salts that serve as starting materials for commercial standards, archived spiked Geochemical Ocean Sections Study (GEOSECS) standards serve as the absolute standard for data produced in our laboratory.

2.2. Results

[7] Barium distributions across the sections are depicted in Figure 2. (Numerical data can be obtained from archives at the National Snow and Ice Data Center in Boulder, Colorado [*Falkner*, 2002].) The Fram Strait transect (section 3) extended from 16°18′W to 8°40′E longitude at $\sim$79°N latitude (Figure 1). The highest Ba concentrations along this section were associated with fresher waters in the southward flowing East Greenland Current (EGC) over the Greenland shelf and slope. The Ba-enriched waters were generally confined to densities (expressed as σ_θ) of 27.0 or less. Departure of the Ba gradient from alignment along σ_θ = 27.0 occurred at shallow depths toward the center of the section, where Ba concentrations became low $\sim$4° east of the outcropping of the σ_θ = 27.0 line. A subsurface Ba

maximum, reaching 70–75 nM, occurred between ∼8°W and 12°W and 25–50 m over the Greenland shelf.

[8] On the eastern part of section 3, waters extending from the surface to ∼1000 m were uniformly low in Ba (40–45 nM). From 1000 m to the bottom, Ba concentrations gradually increased with depth to ∼55 nM while salinity remained fairly homogenous. Profiles along this part of the section are typical for Ba, which has a biogeochemical cycle like that of a hard part nutrient that is regenerated at depth and/or in the sediments [*Chan et al.*, 1977]. East of ∼7°E, temperature and salinity both increased significantly from the surface to 200 m to values near 7°C and 35, respectively, signaling the presence of northward flowing Atlantic water of the West Spitzbergen Current (WSC). This current did not carry a distinctive Ba signature.

[9] As for Ba, the highest dissolved Si concentrations were found over the Greenland shelf on the eastern side of section 3 (Figure 2). A subsurface Si maximum (11 μM) occurred somewhat deeper (≈100 m) than for Ba and was associated with salinities of 33.0–33.5. The higher end of this salinity range is bounded by the σ_θ = 27.0 surface. It is likely that this Si feature is derived from the well-known Si maximum of upper halocline of the Arctic Ocean that originates from inputs at Bering Strait and occurs in the same salinity range [*Schauer*, 2000, p. 30]. The Ba enrichments in this depth range are consistent with such an origin [*Guay and Falkner*, 1997], as are the nitrate plus nitrite (NO$_3$ + NO$_2$ or more simply NO$_3^+$) and phosphate (H$_3$PO$_4$ or more simply P) levels [*Jones and Anderson*, 1986]. Surface waters in the EGC were depleted in Si (to 2 μM) and NO$_3^+$ but not P.

[10] East of ∼3°W, Si was markedly depleted (<1 μM) at the surface and gradually increased with depth to ∼8–10 μM at 1000 m. Phosphate was also markedly depleted (<0.2 μM) in the surface of the WSC at Fram Strait, whereas NO$_3^+$ levels were similar to those in the surface EGC. Oxygen isotopic ratios for seawater (expressed as δ^{18}O relative to Vienna SMOW) along section 3 were generally large and negative over the shelf and positive over the basin. The deeper boundary of δ^{18}O-depleted values conformed quite closely to the outcropping of σ_θ = 27.0, extending farther east than the Ba maximum.

[11] Section 7 ran nearly north-south from 69°22′N, 23°42′W to 66°45′N, 23°W (Figure 1). The four northernmost stations (226–229) were located over the Greenland shelf and slope, while the southernmost stations (233–235) were over the Iceland shelf. As for section 3 the highest Ba concentrations occurred in the freshest and coldest waters flowing southward over the Greenland shelf and were confined to densities σ_θ ≤ 27.0. However, the Ba levels were more uniform and somewhat less concentrated, and the waters were slightly warmer and saltier than at Fram Strait. The associated subsurface (≈75–100 m) Si maximum (8 μM) persisted, with its deeper boundary aligning to σ_θ = 27.0, but was also somewhat less concentrated than at section 3 (Figure 2). Presumably, this results from dilution by the warmer, saltier, and nutrient-depleted waters. This maximum became shallower away from the shelf and extended to 68°30′N latitude. Phosphate and NO$_3^+$ concentrations were also depleted over the east Greenland shelf at this location in contrast to Fram Strait. Oxygen isotope data were unavailable for sections 7 and 8.

[12] Over the Iceland shelf on section 7 an isolated, Ba-enhanced (53 nM) plume centered on station 238, from the surface to ∼100 m, was observed (Figure 2). The plume was associated with cold (−0.6°C) and fresh (33.6) water and was surrounded by much warmer (7.6°C) and saltier (35) water. The levels of Si (7 μM) were also enhanced, but NO$_3^+$ and P were somewhat less concentrated than in surrounding waters (Figure 2). This feature may represent either a filament of EGC water or a local riverine influence. The flow of the Jokulsa River in northern Iceland peaks during the summer months, often exceeding 300 m^3 s^{-1} during this time (Global River Discharge Database, UNESCO). For background seawater levels of 46.5 nM Ba and 35.0 salinity (estimated by averaging measurements above 50 m at neighboring stations) a zero salinity effective riverine end-member of 170 nM Ba is obtained. We were unable to locate data on Ba for major Iceland rivers; however, this estimate falls within the range of usual river water concentrations. In the absence of other information a local riverine source for this plume cannot be ruled out.

[13] Section 8 ran nearly east-west from 66°30′N, 33°39′W to 66°N, 25°W at Denmark Strait (Figure 1). Barium samples were taken only on the eastern half of the section. A Ba maximum (50–55 nM) is present from 28°W to 26°41′W from the surface to ∼100 m (Figure 2). This feature is again largely confined to σ_θ ≤ 27.0 with temperature ranging from −1° to 1°C and salinity 32.5–34 and is associated with elevated Si, P, and NO$_3^+$ levels toward the deeper end of this range. The three easternmost stations over the Iceland shelf (240–242) have quite low Ba contents (40–45 nM). These stations also exhibited high temperatures (7.5°–9°C) and salinity (35) and low Si (3 μM) and P (<0.5 μM) characteristic of the northward flowing Irminger Current.

[14] In general, surface water nutrients and Ba become more depleted along the advective pathways of waters moving from north to south along Greenland and south to north in the east. Likewise, the expression in east Greenland waters of the subsurface halocline layer originating in Bering Strait becomes less pronounced in the southward direction. Gradients in NO$_3^+$ tend to conform largely to the isopycnal structure of the sections, whereas Si, P, and to a lesser extent Ba display significant departures. Clearly, these tracer distributions carry information different from each other and from the salinity fields.

3. Discussion
3.1. Water Mass Composition at Fram Strait

[15] Studies over the past decade have shown that the WSC delivers an important and variable amount of heat with the potential to impact the Arctic Ocean ice cover [*Grotefendt et al.*, 1998; *Steele and Boyd*, 1998; *Swift et al.*, 1997; *Zhang et al.*, 1998]. It has also been appreciated for some time that the EGC conditions a region key to North Atlantic deep water formation [*Aagaard and Carmack*, 1989; *Mauritzen*, 1996a, 1996b; *Swift and Aagaard*, 1981; *Swift et al.*, 1980]. For these reasons it has become a high priority to determine water mass composition and flux and factors controlling their variability at Fram Strait.
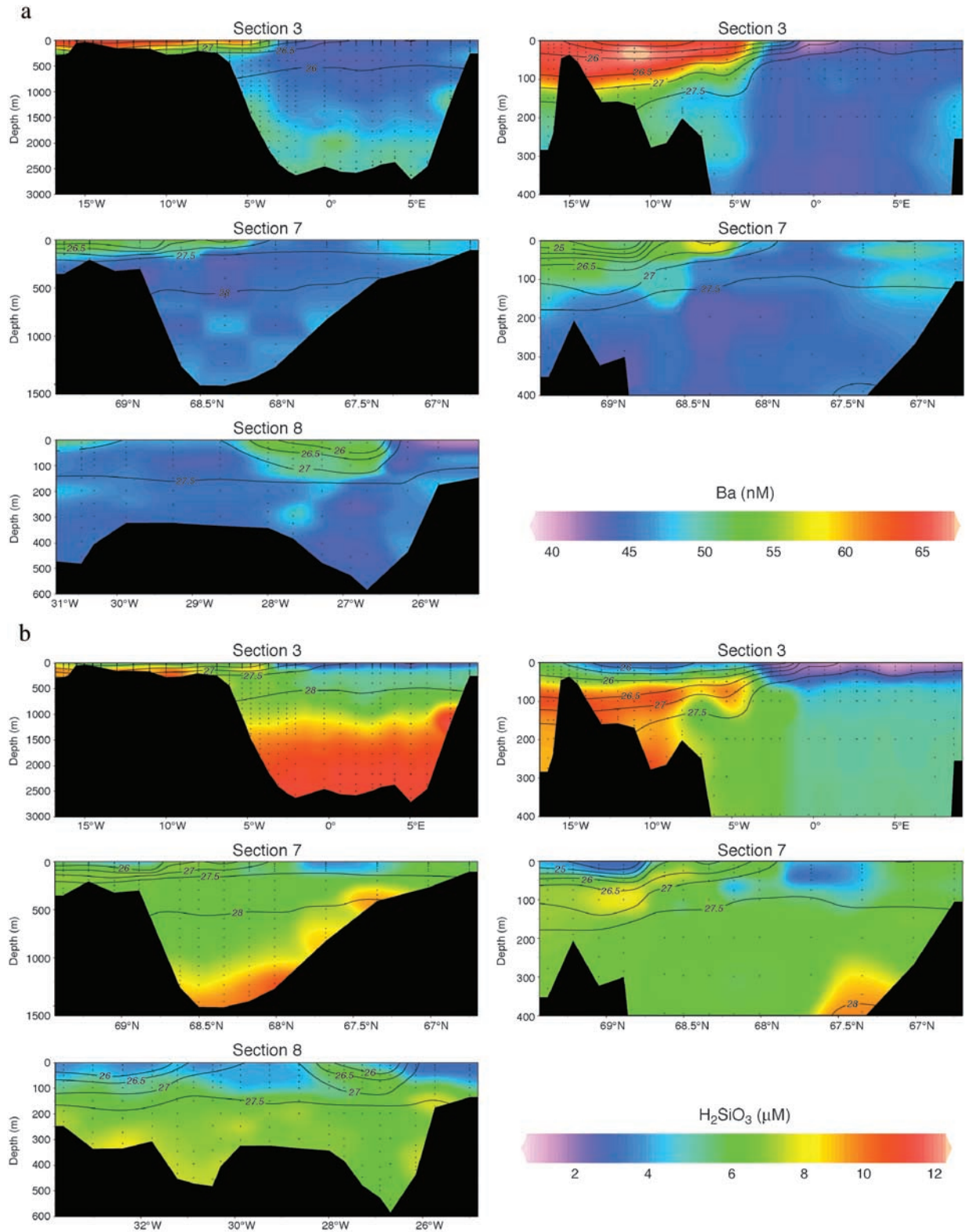
Figure 2. Dissolved property distributions for sections, the locations of which are shown in Figure 1. Sections on the left extend to full depth; sections on the right are expanded to emphasize the upper water column. Contour lines show potential density referenced to the surface or density σ_θ. Small dots indicate measurement locations. Station numbers are given in the caption of Figure 1. For $\delta^{18}O$ along section 3 see *Meredith et al.* [2001]. (a) Dissolved barium. The western portion of section 8, where no Ba data were available, is excluded from the plot. (b) Dissolved siliceous acid. (c) Nitrate plus nitrite. (d) Dissolved phosphate.
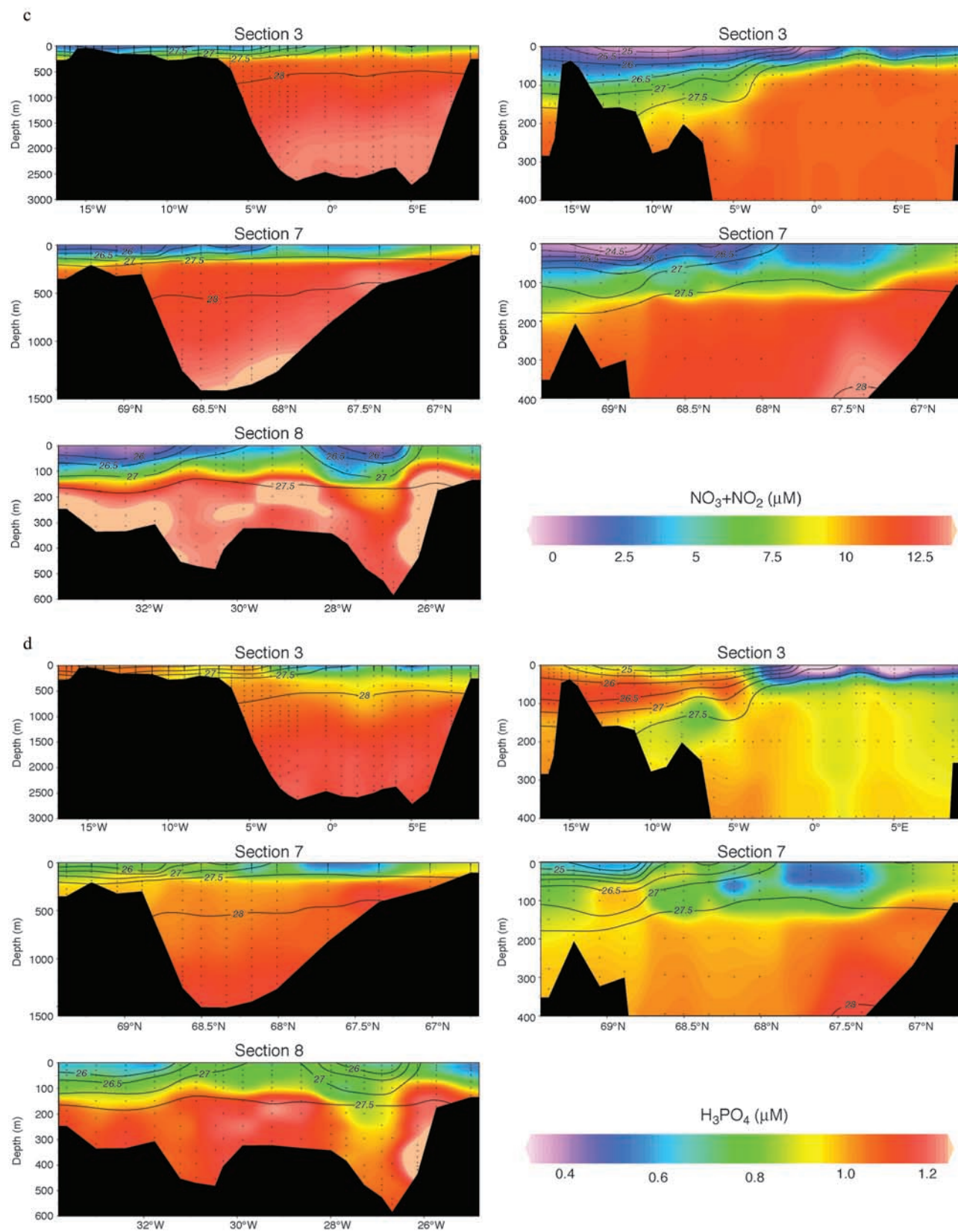
Figure 2. (continued)

Table 1. End-Member Values and Uncertainties for Water Mass Composition Analysis[a]

	Ice Melt	North American Runoff	Eurasian Runoff	Arctic Seawater	Pacific Seawater	Atlantic Seawater
Salinity, on PSS[b]	3	0	0	34.2	NA	NA
$\delta^{18}O$, ‰ Vienna SMOW	1	−20.3	−17.6	−0.13	NA	NA
Ba, nM	5.4	520	120	57	NA	NA
NO_3^+:P slope	14.9	12.4	17.5	NA	12.4	17.5
NO_3^+:P intercept ($NO_3^+ = 0$), μM	−6.8	19.7	−4.6	NA	−10.6	−3.1
Estimated uncertainty, %	5	3	6	NA	14	14

[a]See section 3.1 for details. NA is not applicable.
[b]PSS is practical salinity scale.

The data reported here are part of an intensified international effort to monitor fluxes at Fram Strait [e.g., *Fahrbach et al.*, 2001].

[16] Several tracers have been applied to deciphering the origins of water masses transiting Fram Strait. Distributions of $\delta^{18}O$ have been used to determine the presence of river water and precipitation (which combined are termed meteoric waters) versus sea ice melt (or formation) [*Bauch et al.*, 1995; *Meredith et al.*, 2001; *Östlund and Hut*, 1984]. Contrary to prior assumptions, recent findings suggest that the flux of meteoric water may exceed the flux of sea ice out of Fram Strait by up to a factor of 2 [*Meredith et al.*, 2001]. Significant uncertainties remain, however, since the meteoric flux was estimated from hydrographic sections conducted in the fall of 1997 and 1998 that were extrapolated to a year. No velocity data were available from over the Greenland shelf, so this highly freshened component was not included in the estimates. The percentages of meteoric water to sea ice melt did occur in an approximately 2:1 relationship, however. It should be noted for the sake of comparison to this work that Meredith et al. did not explicitly consider a Pacific contribution to the isotopic signature, so their ''meteoric'' component effectively includes freshening from runoff and precipitation that occurs in the North Pacific south of Bering Strait.

[17] Phosphate (P) to nitrate plus nitrite (NO_3^+) relationships have been used to distinguish Pacific water originating at Bering Strait from Atlantic water [*Jones et al.*, 1998, 2003]. Denitrification occurring in the vicinity of Bering Strait generates a relative surfeit of P in Pacific waters. Within the Arctic, nutrients tend to be stripped from surface waters in Redfield proportions. Thus the NO_3^+ versus P relationships of purely Pacific and Atlantic waters evolve along similar slopes but are offset by ∼1 μM P in the Arctic. Provided there are no additional complications, mixtures plot between these lines, and the proportion of the Pacific and Atlantic contributions can be uniquely determined from the relationships governing the ''pure'' end-members. In practice, it has been assumed until now that runoff carries an Atlantic-like signature, so the runoff was implicitly combined in that term. Perturbations of the nutrient ratios by sea ice melt and precipitation were assumed to be negligible. On the basis of this approach, upward of 90% Pacific water was reported in the upper EGC for hydrographic sections occupied across Fram Strait in the fall seasons of 1997–1999 [*Jones et al.*, 2003].

[18] The proportion of Pacific water in the upper EGC is not always so high. When we apply the same data treatment as reported by *Jones et al.* [2003] to June 1987 observations

from the ARK-XIV/2 expedition at 79.8°N, 10°W to 8°W, a maximum of only 52% Pacific water is seen at the surface over the Greenland shelf. Whether fluctuations in the proportion of Pacific water in the EGC reflect seasonal and/or interannual variability remains to be determined. It is clear, however, that Pacific water can be transported with very little dilution all the way from Bering Strait to Fram Strait.

[19] To learn more about the pathway of this Pacific water and water mass composition in Fram Strait, we now consider multiple tracers, including Ba, $\delta^{18}O$, NO_3^+:P relationships, and salinity for ARK-XIV/2 section 3. Combining the four tracers along with volume conservation allows quantification of five unknowns, namely, Atlantic water, Pacific water, ice melt (or extraction), North American river runoff, and Eurasian river runoff contributions. We adopted a two-step process in order to accommodate the nonlinear treatment of the nutrient data. First, equations conserving volume, salinity, $\delta^{18}O$, and Ba on the basis of assigned end-members (Table 1) were used to derive ice melt, North American river runoff, Eurasian river runoff, and a combined Atlantic and Pacific seawater component we shall term Arctic seawater. Next, NO_3^+:P relationships were applied to this Arctic seawater component to distinguish Atlantic and Pacific contributions, with each of the two sources constrained to contribute between 0 and 100% of the seawater. Negative values of ice meltwater mass represent a net removal of water via ice formation.

[20] The end-member values in Table 1 were selected specifically for application in the Fram Strait region. Because of the incorporation of brine cells, fresh sea ice typically has salinities upward of 6 [*Weeks and Ackley*, 1986]. It is likely that the ice exiting Fram Strait has aged enough to experience brine drainage, so we assign a lower salinity of 3. The $\delta^{18}O$ for sea ice was derived from an area-averaged, Arctic surface seawater value of −1.6‰. A fractionation factor of 2.6‰ was added to this value following *Ekwurzel et al.* [2001]. Values for the seawater component were derived from a flow-weighted average of Bering Strait and WSC observations using the measurement-based volume flux values listed in Table 2. The $\delta^{18}O$ for runoff was derived from weighting data reported for individual rivers [*Ekwurzel et al.*, 2001] by their average annual discharge. Values of Ba in North American and Eurasian runoff are derived from flow-weighted riverine end-members that include a desorbed component [*Guay and Falkner*, 1998]. Values for sea ice Ba are derived assuming that Ba behaves conservatively with salinity in the freezing process. Seawater freezing experiments show

Table 2. Measurement-Based and Steady State-Model Flux Estimates and Their Uncertainties, as Defined in Equations (2)–(6)[a]

	Estimates				Uncertainties			
	Q, Sv	H, Sv °C	S^{b}, Sv	B^{c}, mol s^{-1}	σ_{Q}, Sv	σ_{H}, Sv °C	σ_{S}, Sv	σ_{B}, mol s^{-1}
Canadian archipelago	−1.37	1.06	0.87	−11.0	0.22	0.22	0.86	8.4
	−1.44	1.12	0.94	−14.0	0.21	0.22	0.81	7.6
Barents Sea	1.59	9.50	0.95	−10.6	0.26	3.63	0.22	6.6
	1.46	9.08	0.85	−11.0	0.26	3.52	0.22	6.3
Bering Strait	0.83	−0.38	−1.58	16.0	0.12	0.34	0.26	5.5
	0.80	−0.37	−1.54	14.7	0.12	0.34	0.26	5.3
Fresh water	0.13	0.63	−4.30	15.5	0.04	0.33	1.52	5.9
	0.11	0.54	−3.65	14.1	0.04	0.31	−1.21	4.8
Fram Strait								
Ice	−0.07	0.20	2.14	0.0	0.01	0.08	0.44	0.3
	−0.07	0.21	2.15	0.0	0.01	0.08	0.44	0.3
EGC Polar Water	−1.27	0.15	1.23	2.3	0.26	1.81	1.78	11.0
	−1.34	0.08	1.34	−1.7	0.25	1.80	1.29	9.4
EGC Atlantic Water	−1.73	−0.60	−0.86	11.5	0.53	1.02	0.27	6.0
	−2.02	−0.80	−1.07	13.1	0.47	1.02	0.25	5.7
EGC Deep Water	−0.97	0.55	−0.50	2.7	0.20	0.25	0.14	3.1
	−1.02	0.58	−0.53	2.5	0.20	0.25	0.14	3.0
WSC Atlantic Water	3.94	12.20	2.20	−23.6	0.94	9.61	0.73	11.2
	2.79	8.89	1.13	−16.1	0.57	7.27	0.59	9.2
WSC Deep Water	0.75	−0.64	0.38	−1.0	0.12	0.11	0.10	2.6
	0.73	−0.63	0.37	−1.2	0.12	0.11	0.10	2.6
Surface heat flux								
Basin		0.00				7.44		
		−0.98				5.63		
Barents		−13.94				6.27		
		−14.72				5.15		
Canada basin polynyas		−1.34				0.47		
		−1.35				0.47		
Eurasian basin polynyas		−0.56				0.20		
		−0.56				0.20		
Shelf other		0.00				8.37		
		−1.10				5.89		
Total[d]	1.82	6.82	0.55	0.17	1.19	16.59	2.68	2.19
	0.01	0.00	0.00	0.03	0.89	12.77	2.13	1.92

[a]First entry is measurement-based estimate; second entry is steady state-model flux estimate.
[b]Salinities are expressed as a deviation from a mean of 34.4 on the unitless PSS; $S = Q(s − 34.4)$.
[c]Barium is expressed as a deviation from a mean of 52.7 nM; $B = Q(b − 52.7)$.
[d]Total denotes net for flux estimates and norm for uncertainties.

this to be true within analytical uncertainties (K. Falkner and D. Meese, unpublished data, 1995):

$$\text{Ba}_{\text{ice}} = \frac{S_{\text{ice}} \times \text{Ba}_{\text{surface}}}{S_{\text{surface}}}, \qquad (1)$$

where S_{ice} is the assigned salinity of Fram Strait sea ice. The relationship between Ba and salinity varies in Arctic Ocean surface waters, so values in multiyear sea ice may not reflect local surface water conditions. As shown below, the calculations are not particularly sensitive to the assigned values, so for simplicity we use average Arctic Ocean surface values of Ba and S in evaluating this expression.

[21] To determine the Atlantic and Pacific water contributions to the seawater component, we adapted the previously reported NO$_3^+$:P approach [*Jones et al.*, 1998, 2003]. Linear regression parameters for the NO$_3^+$:P relationships assigned are listed in Table 1. Atlantic and Pacific water NO$_3^+$:P relationships were taken from measurements over the St. Anna Trough and the Chukchi shelf and slope, respectively [*Jones et al.*, 1998]. Runoff contributions to NO$_3^+$:P relationships were taken into account explicitly on the basis of data compiled for the lower reaches of Eurasian rivers by *Gordeev et al.* [1996] and North

American rivers by *Mackenzie-River-Basin-Committee* [1981]. To account for subsequent biological activity, it was assumed that upon delivery to the shelf the North American rivers follow the same NO$_3^+$:P slope as Chukchi shelf water. Similarly, the Eurasian runoff NO$_3^+$:P slope was assumed to be the same as for St. Anna Trough water. The NO$_3^+$:P relationship of sea ice is set by assuming that sea ice is composed of equal parts of Atlantic and Pacific water. Since the sea ice flux is small compared with the flux of Atlantic and Pacific water, this assumption does not significantly affect the results.

[22] The sensitivity of the calculations was investigated by systematically varying the tracer values assigned to the end-members. Ice melt and the North American and Eurasian runoff components depend most strongly on the Arctic seawater tracer values. Ice melt and Eurasian runoff fractions are highly sensitive to the δ^{18}O of the seawater end-member. Increasing the seawater δ^{18}O from −0.5 to 0.5 increases the Eurasian runoff and simultaneously decreases the ice melt by 5% of the total water mass. The fraction of North American runoff is most sensitive to the Arctic seawater Ba. Decreasing the Ba seawater from 56.6 to 46.6 nM increases the contributions from North American rivers and Pacific water by 2% and 5% of the total water mass, respectively, and decreases the Eurasian
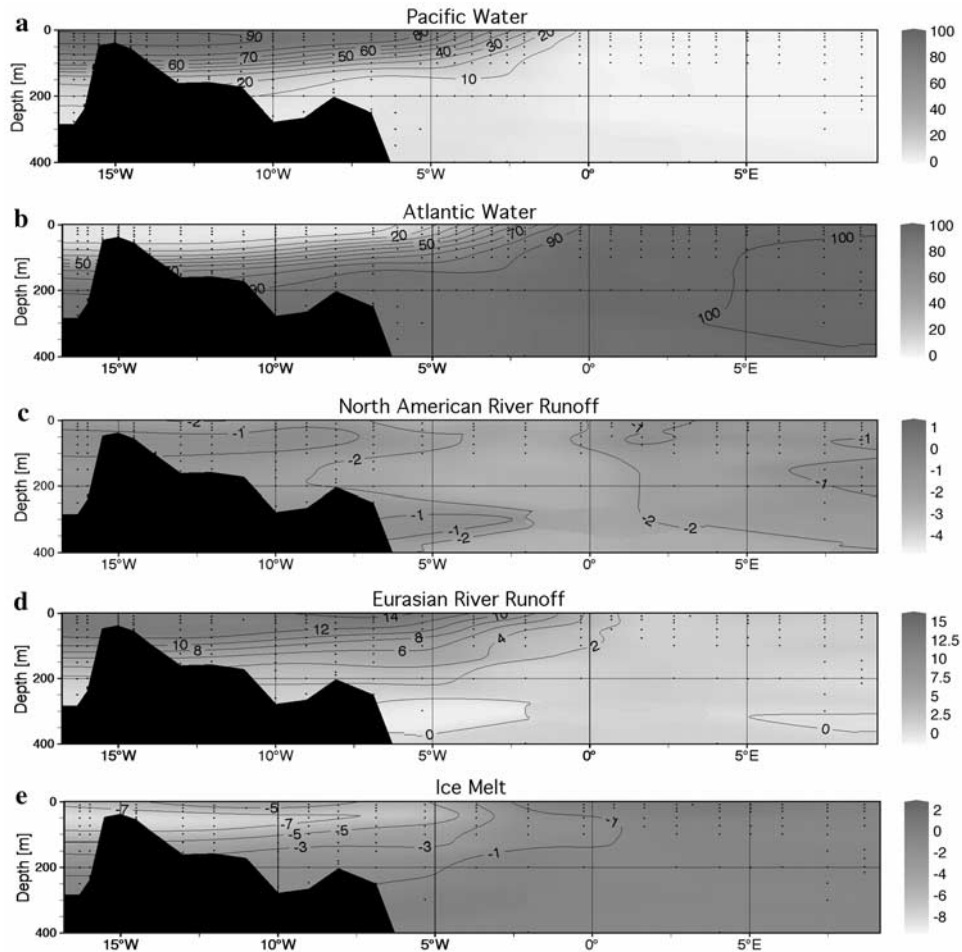
Figure 3. Water mass composition for the upper water column of Fram Strait section 3: (a) Pacific Water, (b) Atlantic Water, (c) North American river runoff, (d) Eurasian river runoff, and (e) ice melt. Shading and contour lines show the percentage of the total water mass accounted for by each source. Note the different scales used for shading. Estimated uncertainties associated with each of the components are given in Table 1.

rivers and Atlantic water contributions by 3% and 5%, respectively. Additional uncertainty accumulates from the NO_3^+:P assignments. A range of possible NO_3^+:P relationships was obtained by fitting the largest and smallest possible slopes to NO_3^+ versus P data at the Chuckchi shelf and St. Anna Trough. Adjusting the assigned NO_3^+:P relationships within this range causes the Atlantic and Pacific water fractions to vary by ~10% of the total water mass.

[23] Varying the assigned tracer values within the error bars gives a realization vector for each water mass component. Error bounds for each of the components were then determined by taking the norm (defined as the square root of the sum of the squares) of the realization vectors. Uncertainties estimated in this way for each of the fractions of each of the components are summarized in Table 1.

[24] Analyzed by our approach, the distribution of Pacific water in the EGC (Figure 3a) is qualitatively similar to that reported by *Jones et al.* [2003]. However, our Pacific water fraction extends neither as deep nor as far east as reported by Jones et al. and is ~10% lower at the surface. The difference is due largely to the presence of Eurasian river water, which contributed up to 15% of the water in some locations (Figure 3d).

[25] Interestingly, the North American runoff fraction was negligible for the entire section (Figure 3c), being always less than its standard error. Note that the negative values seen here are smaller than the standard error and therefore are indistinguishable from zero. The standard error for the Eurasian river runoff contribution is also high, ±6% relative to a maximum value of 15%.

[26] The lack of North American runoff is somewhat surprising because North American river-influenced surface waters and the upper halocline Si maximum are colocated throughout the Beaufort Gyre [*Guay and Falkner*, 1997]. In Fram Strait section 3, however, Eurasian river water at the surface accompanied subsurface Si maximum and elevated Ba that originate in Bering Strait. Thus, within the Arctic interior, surface waters in the Beaufort Gyre can be displaced by transpolar drift waters that bear Eurasian runoff.

[27] Under these circumstances, North American runoff must be stored in the Beaufort Gyre and/or must drain through passages of the Canadian archipelago. Analyzed in the same way as the Fram Strait data, hydrographic sections
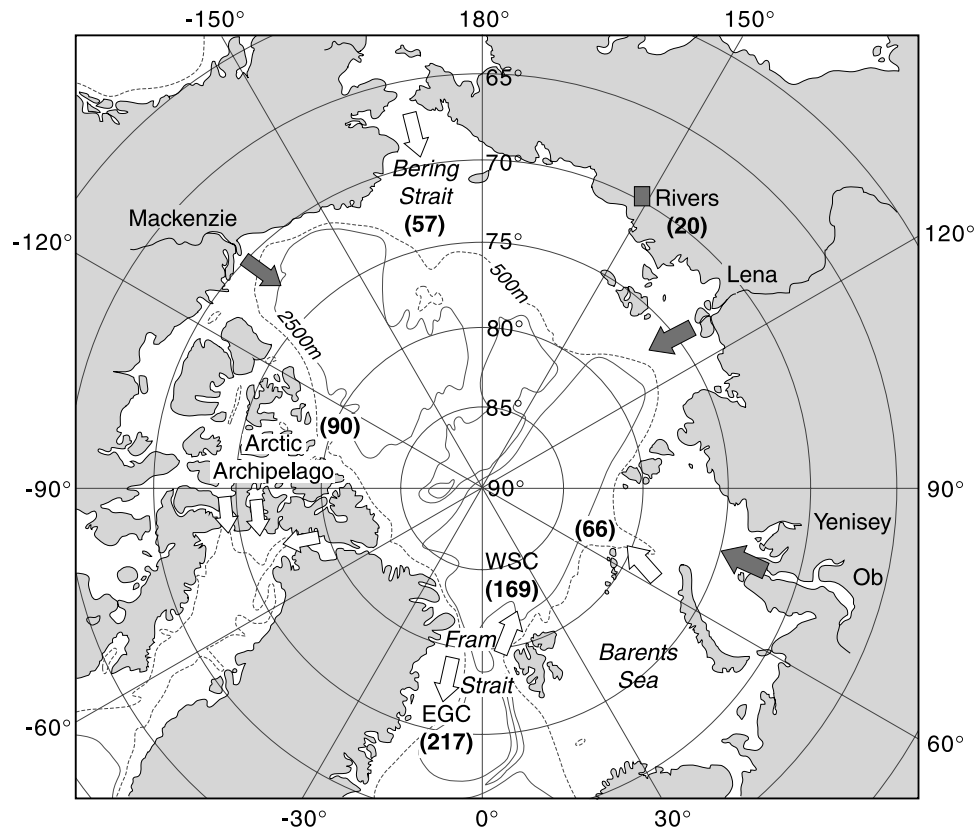
Figure 4. Map denoting locations of the major water exchanges and summarizing the best fit conservative Ba budget of the Arctic Ocean. Volume, salt, and heat are also conserved in this budget. Barium fluxes are in units of mol s^{-1}. Smoothed bathymetric contours at 500 and 2500 m were derived from the GEBCO database.

in August 1997 show a mixture of Eurasian and North American river water flowing through the easternmost passage at Smith Sound but exclusively North American runoff in Jones Sound and Barrow Strait (Falkner et al., manuscript in preparation, 2003). We speculate that the proportion of Eurasian versus North American runoff draining through Smith Sound and possibly Fram Strait is a function of larger-scale atmospheric pressure patterns that determine the positioning of the transpolar drift. The transpolar drift as represented in drifting buoys tracked by satellite and models displays seasonal and interannual variability that appears to be linked with larger-scale atmospheric pressure patterns [*Proshutinsky and Johnson*, 1997; *Rigor et al.*, 2002].

[28] Ice formation (negative ice melt) signatures exceeding 8% in some locations occurred over the shelf at ~50 m (Figure 3e). The remainder of the shelf water displayed less intense ice formation (1−3%). These signatures do not necessarily implicate local ice formation, as they could have been inherited from regions upstream. East of the shelf, ice melt was generally positive but contributed <2% to the total water mass composition.

3.2. Dissolved Barium Budget for the Arctic Ocean
3.2.1. Overview

[29] Over the past decade a database has been amassed that allows a first-order description of the distribution of Ba in the basins of the Arctic Ocean and at all of its major passageways. In principle, information contained in the Ba distributions, as summarized in section 1, could provide unique constraints for circulation models of the Arctic Ocean. To use Ba to test either numerical modeling approaches or inverse modeling schemes, knowledge of its boundary conditions is a prerequisite. Ideally, observations capturing the spatial and temporal variability of Ba fluxes at the boundaries would be used to construct an Arctic Ba budget. Such detailed observations are lacking; however, Ba measurements do exist for all of the major passageways (Figure 4). On the basis of these measurements we shall construct a preliminary budget for Ba in the Arctic Ocean.

[30] For the purposes of this exercise the Arctic Ocean is defined to be seawater and ice in the Canadian and Eurasian basins, their surrounding shelves, and the Barents Sea (Figure 4). Our approach is analogous to that of *Goldner* [1999], who obtained a budget conserving heat, salt, and volume (as an approximation to mass) for the Arctic Ocean via inverse techniques. The input to *Goldner*'s [1999] model consisted of uncertainty-weighted averages of a number of previous flux estimates reported in the literature from 1975 to 1997. Such an approach is preferable to selecting only the most recent or well-determined flux estimates because the Arctic system is dynamic over the interannual to decadal timescales.

[31] In principle, the 1975–1997 time frame used by *Goldner* [1999] captures two major modes of atmosphere-ocean variability [*Proshutinsky and Johnson*, 1997]. In practice, the relationships between boundary fluxes and system variability have yet to be characterized. Since it is unlikely that all boundary fluxes are equally well represented by existing estimates, the model will need refining as this information becomes available. In the meanwhile, we adopted estimates of volume flux, temperature, and salinity from *Goldner* [1999] with the exception of Fram Strait, where temperature and salinity were estimated from observations during the ARK-XIV/2 cruise as described in section 3.2.2. Barium fluxes were estimated as described in section 3.2.2.

3.2.2. Ba Flux at Fram Strait

[32] Data for Ba at Fram Strait were only available for the ARK-XIV/2 cruise of 1998. Velocity fields from current meter moorings deployed at Fram Strait at the same latitude as the ARK-XIV/2 stations [*Fahrbach et al.*, 2001] were used to define the locations of the EGC and the WSC. In order to account for variation with depth of water properties and north-south volume transport the EGC was divided into three components: EGC Polar Water (0–250 m), EGC Atlantic Water (250–1000 m), and EGC Deep Water (>1000 m). The WSC was divided into WSC Atlantic Water (0–1000 m) and WSC Deep Water (>1000 m).

[33] Barium, temperature, and salinity values were assigned to each region by taking a volume average of the observations with uncertainties equal to the standard deviation of the observations. The EGC Polar Water captures the region of relatively high Ba (50–65 nM) near the surface but also includes lower Ba values (45 nM) on the eastern end of the EGC core beneath the surface. This variability leads to a high Ba standard deviation in the EGC polar water. Both regions of Atlantic Water were depleted in Ba (42–45 nM), and the Deep Water division captures the Ba regeneration (~50 nM) near the ocean floor. The EGC, as defined by large mean velocities, encompassed the region east of station 70 and west of station 60, and the WSC occurred at locations east of station 41.

3.2.3. Ba Input at Bering Strait

[34] Measurements of Ba have been published for a September 1992 section across Bering Strait [*Falkner et al.*, 1994]. At that time it was determined that Ba concentrations of 65–73 nM typified waters flowing northward in the strait. Measurements during the summer-fall time frame in subsequent years generally reinforce these findings (K. Falkner, unpublished data, 1993, 1999, 2000) with higher values (100–125 nM Ba) sometimes occurring in thin layers near the bottom. The average Ba of all available measurements on waters flowing into Bering Strait is 72 ± 7 nM.

3.2.4. Ba Input in Runoff

[35] Riverine Ba fluxes directly to the Arctic Ocean have been estimated from measurements in the 1990s for eight Arctic rivers: the Mackenzie, Yenisey, Lena, Ob, Pechora, Indigirka, Pyasina, and Yana [*Guay and Falkner*, 1998]. These rivers contribute ~65% of the estimated total river water flux of 3300 km^3 yr^{-1} to the Arctic [*Aagaard and Carmack*, 1989]. As occurs commonly at lower latitudes, transects through the estuaries of these rivers showed signs that Ba is both delivered directly in river water and desorbed from clays. Effective riverine end-member Ba values were estimated by extrapolating to zero salinity from the linear portion of the salinity versus Ba curve. These effective end-members were then multiplied by the average annual discharge to obtain a first-order estimate of Ba fluxes from these rivers [*Guay and Falkner*, 1998, Table 2]. The flux-weighted average Ba concentration from these rivers was taken to represent all Arctic river input.

[36] Multiple uncertainties arise from this approach. It is unclear, for example, what the magnitude of the seasonal variability of Ba in the rivers might be. River water Ba data for Eurasia were obtained exclusively in the late summer and autumn after the peak flow season (June–July), and the data did display some interannual variability. Because of freezing in their drainages these rivers experience tenfold to sixtyfold flow variations seasonally and interannual variations of 5–20% [*Carmack*, 1990]. Such variability can be expected to impact suspended sediment load and Ba contents. Unlike the Eurasian rivers, the Mackenzie's flow is modulated by the occurrence of sizable lakes in its drainage, so its flow varies by less than a factor of 10 throughout the year. The Mackenzie samples taken in one winter (1994) and a subsequent summer (1996) did not differ appreciably in their Ba contents. It is also unclear whether eight rivers adequately represent unmeasured circum-Arctic drainage. Lacking data to address these issues, we take a simple approach and assign a 10% uncertainty to the composite riverine Ba concentration and 40% uncertainty to the Ba flux estimate.

3.2.5. Ba Output to the Canadian Archipelago

[37] Barium concentrations were measured at Jones Sound, Smith Sound, and Barrow Strait as part of the Surface Heat Budget of the Arctic Ocean/Joint Ocean Ice Studies 1997 Canadian Coast Guard Ship *Louis S. St. Laurent* expedition (Falkner et al., manuscript in preparation, 2003). Information on the currents at the time of these sections is not available; hence we numerically averaged the Ba measurements. The average (±1 standard deviation) of 65 Ba observations in Jones Sound was 65.0 ± 4.1 nM, the average of 66 observations in Smith Sound was 58.4 ± 5.6 nM, and the average of 81 observations in Barrow Strait was 64.6 ± 4.3 nM. These values were weighted by estimated proportioning of the flow of 20%, 40%, and 40% through Jones Sound, Smith Sound, and Barrow Strait, respectively [*Fissel et al.*, 1988], to obtain an estimated Ba of 62 nM for the combined archipelago through flow. An uncertainty of 10% was assigned to this value.

3.2.6. Budget Computations

[38] We shall adopt a notation using lowercase letters for tracer quantities (t is temperature, s is salinity, o is δ^{18}O, and b is Ba) and uppercase letters for tracer fluxes (H is heat flux, S is salinity flux, O is δ^{18}O flux, and B is Ba flux). Tracer quantities are multiplied with volume fluxes Q in order to estimate tracer fluxes

$$H = tQ, \tag{2}$$

$$S = sQ, \tag{3}$$

$$O = oQ, \tag{4}$$

$$B = bQ. \tag{5}$$

Table 3. Barium Budget Terms[a]

Location	Prior Estimate		Conservative Estimate	
	Ba, nM	B, mol s^{-1}	Ba, nM	B, mol s^{-1}
Canadian archipelago	60.8 ± 6.0	−83.1 ± 8.4	62.4 ± 5.1	−89.7 ± 7.6
Barents Sea	46.0 ± 4.0	73.1 ± 6.6	45.2 ± 4.1	66.1 ± 6.3
Bering Strait	72.0 ± 6.0	59.6 ± 5.5	71.1 ± 6.0	56.6 ± 5.3
Fresh water	177 ± 17	22.1 ± 5.9	186 ± 11	19.7 ± 4.8
Fram Strait				
Ice	52.7 ± 5.0	−3.6 ± 0.3	52.7 ± 5.0	−3.6 ± 0.3
EGC Polar Water	50.9 ± 8.7	−64.4 ± 11.0	54.0 ± 7.0	−72.5 ± 9.4
EGC Atlantic Water	46.1 ± 2.8	−79.8 ± 6.0	46.2 ± 2.4	−93.1 ± 5.7
EGC Deep Water	50.0 ± 3.1	−48.6 ± 3.1	50.2 ± 2.9	−51.1 ± 3.0
WSC Atlantic Water	46.7 ± 2.5	184 ± 11	46.9 ± 3.1	131 ± 9
WSC Deep Water	51.4 ± 3.4	38.5 ± 2.6	51.1 ± 3.5	37.5 ± 2.6

[a]See section 3 for details.

(See *Goldner* [1999] for details on the treatment of heat fluxes associated with advection, ice, and surface exchange.)

[39] Given variances in the volume flux Q and tracer quantities (Table 2), the variances and covariances of the tracer fluxes can be estimated. Assuming that the tracer quantities are uncorrelated to the volume flux estimates and to each other, the expressions of the following form can be derived:

$$\text{var}(B) \equiv (\sigma_B)^2 \cong b^2 (\sigma_Q)^2 + Q^2 (\sigma_B)^2 \qquad (6)$$

$$\text{cov}(BQ) \cong b(\sigma_Q)^2. \qquad (7)$$

[40] Once major fluxes to and from the Arctic and their error bounds are determined, it is desirable to determine whether the Arctic can be considered to be in steady state. Following *Goldner* [1999], we pose this question as an inverse problem: Determine the set of tracer fluxes that satisfies the steady state constraint while keeping the fluxes as close as possible to their estimated values and within their estimated error limits. Simultaneous consideration of volume, heat, salinity, and Ba can be summarized by the following system of equations:

$$
\begin{aligned}
\hat{Q}_i + e_{Q_i} &= Q_i & \sum_i \hat{Q}_i + e_{Q_c} &= 0 \\
\hat{H}_i + e_{H_i} &= H_i & \sum_i \hat{H}_i + e_{H_c} &= 0 \\
\hat{S}_i + e_{S_i} &= S_i & \sum_i \hat{S}_i + e_{S_c} &= 0 \\
\hat{B}_i + e_{B_i} &= B_i & \sum_i \hat{B}_i + e_{B_c} &= 0,
\end{aligned}
\qquad (8)
$$

where i is an index of the flux sources, hats denote unknown flux terms to be determined, e_i denotes the difference between the conservative budget flux and the flux estimate, and e_c is the deviation of the solution from perfect conservation. The goal is to solve this system for the unknowns that minimize the sum of the squared deviations. Before solving, the system is weighted by the estimated covariance matrix so that fluxes with larger estimated errors will be adjusted more freely. The prior errors in the volume, heat, and salt conservation statements are set to 0.01 of the respective units in Table 2. Not knowing how well determined the Ba flux terms are, we assigned a larger error of 0.3 to the Ba conservation statement. The Ba and salinity flux values listed in Table 2 have been computed by subtracting Arctic-wide mean values from the tracer quantities, then multiplying by the volume flux.

[41] Each conservation statement error is assumed to be uncorrelated to the prior flux errors. Note, however, that the net flux conservation statements will introduce correlations between the various flux terms that were previously assumed to be independent. Such correlations will need to be taken into account in any future modeling effort based on the conservative fluxes.

[42] The least squares solution yielded a set of conservative flux values within the assigned errors (Table 2). Statistical validity of the least squares solution was confirmed by a chi-square goodness-of-fit test. The chi-square for the inverse with 4 degrees of freedom was 2.40, and the probability of obtaining a larger chi-square was 0.66. This implies a better-than-average fit and suggests that the hypothesis of a steady state budget is consistent with the observed flux values and the assigned errors.

[43] The largest adjustments to volume flux were made for the WSC Atlantic Water and the EGC Atlantic Water, which had been assigned the largest uncertainties. The WSC Atlantic Water volume flux decreased by 1.1 Sv, and the EGC Atlantic Water volume flux decreased by 0.3 Sv. Very little adjustment was made to the temperatures assigned to the fluxes. The heat budget was balanced largely with adjustments to the more uncertain surface heat flux terms. The largest adjustment to salinity was made for WSC Atlantic Water that was decreased by 0.15 (salinity expressed on the unitless practical salinity scale) from the initial estimate. Other changes to salinities were negligible. Small adjustments to Ba were made to fresh water and EGC Polar Water, which were increased by 8.6 and 3.1 nM, respectively (Table 2). Table 3 lists the values of Ba and Ba flux before and after enforcing conservation.

[44] A recent study has reported a significantly larger volume flux through Fram Strait than many previous estimates. *Fahrbach et al.* [2001] report transports of 9.5 ± 1.4 Sv for the WSC and 13.7 ± 1.7 Sv for the EGC. When we substitute these estimates for the Fram Strait estimates of *Goldner* [1999], the total volume flux for all inflows and outflows becomes −3.1 Sv, indicating a net loss of volume from the Arctic. To determine the feasibility of a volume-conserving budget from this set of volume fluxes, a least squares fit was attempted with the constraint of volume conservation. A conservative budget within the

assigned errors could be obtained, but each term had to be adjusted close to the upper error bound in order to compensate for the large negative total volume flux implied by the initial estimates. The chi-square for the calculation with 1 degree of freedom was 3.96, with a chi-square probability of 0.05, indicating that the conservative budget is not a statistically likely fit to the data.

[45] In this scenario either the given combination of volume flux estimates is not accurate, the hypothesis of a volume-conserving budget is incorrect, or the error assigned to the estimates is too small. The first of these possibilities is probably the largest source of error. If the volume inflow at the Barents Sea is correlated to the inflow through the WSC, then the Barents volume flux estimate of *Goldner* [1999] cannot be expected to tally properly with the late 1990s Fram Strait volume fluxes estimated by *Fahrbach et al.* [2001]. A larger corresponding volume inflow through the Barents Sea could make up the deficit to produce a volume-conserving budget. Further progress awaits the results of simultaneous monitoring of fluxes and their variability at the Arctic gateways.

4. Conclusions

[46] *Jones et al.* [1998] discussed two possible pathways whereby Pacific water can reach Fram Strait. One branch follows the Alaskan and Canadian coastlines and enters Fram Strait at the northeastern tip of Greenland. The second branch enters the East Siberian Sea, mixes with water present there, and is borne by the transpolar drift across the Arctic to Fram Strait. Our findings, notably the lack of any evidence of Mackenzie River water in the EGC, support the predominance of this second pathway at the time of our sampling in Fram Strait. It remains to be determined whether North American runoff can be found in the EGC on a seasonal or interannual basis. *Jones et al.* [1998] suggested that when Pacific water enters the East Siberian Sea, it mixes with Atlantic water coming from the west. However, our analysis shows very little Atlantic water mixed in the Pacific-rich portion of the EGC. Instead, Pacific water seems to have mixed with a significant amount of Eurasian river water.

[47] The Ba flux estimates presented in section 3.2.1 should be viewed as preliminary. No Ba time series data are available, so uncertainties discussed here are based largely on the spatial variability of the observations. On the basis of the biogeochemical behavior of Ba, however, it seems likely that temporal variations would roughly average out over an annual scale. To improve the confidence in the Ba budget, time variability of Ba fluxes over the annual to decadal timescale should be obtained.

[48] Even with this uncertainty, there is reason to believe that this budget may be a reasonable first-order one for Ba and that it behaves largely conservatively. Despite allowing a fairly large amount of potential adjustment in the Ba terms, a conservative budget was produced that required only slight adjustments in Ba fluxes (well within assigned error). We caution that conservation may not hold at finer than basin-wide spatial resolution within the Arctic since processes can generate large-scale balance while not conserving Ba locally. We conclude that it would be justifiable at this juncture to undertake exploratory Arctic Ocean-scale modeling efforts based on the assumption that Ba is a conservative tracer.

References

Aagaard, K., and E. C. Carmack, The role of sea ice and other fresh water in the Arctic circulation, *J. Geophys. Res.*, *94*(C10), 14,485–14,498, 1989.

Bauch, D., P. Schlosser, and R. Fairbanks, Freshwater balance and sources of deep and bottom water in the Arctic Ocean inferred from the distribution of $H_2^{18}O$, *Prog. Oceanogr.*, *35*, 53–80, 1995.

Carmack, E. C., Large-scale physical oceanography of polar oceans, in *Polar Oceanography, Part A: Physical Science*, edited by W. O. Smith, pp. 171–222, Academic, San Diego, Calif., 1990.

Chan, L. H., D. Drummond, J. M. Edmond, and B. Grant, On the barium data from the Atlantic GEOSECS expedition, *Deep Sea Res.*, *24*, 613–649, 1977.

Ekwurzel, B., P. Schlosser, R. A. Mortlock, R. G. Fairbanks, and J. H. Swift, River runoff, sea ice meltwater, and Pacific water distribution and mean residence times in the Arctic Ocean, *J. Geophys. Res.*, *106*(C5), 9075–9092, 2001.

Fahrbach, E., *The Expedition ARKTIS XIV/2 of the Research Vessel "Polarstern" in 1998*, 114 pp., Alfred Wegener Inst. for Polar and Mar. Res., Bremerhaven, Germany, 1999.

Fahrbach, E., J. Meincke, S. Østerhus, G. Rohardt, U. Schauer, V. Tverberg, and J. Verduin, Direct measurements of volume transports through Fram Strait, *Polar Res.*, *20*(2), 217–224, 2001.

Falkner, K., Fram Strait and Denmark Strait dissolved barium concentrations, http://nsidc.org/arcss/, Natl. Snow and Ice Data Cent., Boulder, Colo., 2002.

Falkner, K. K., R. W. Macdonald, E. C. Carmack, and T. Weingartner, The potential of barium as a tracer of Arctic water masses, in *The Polar Oceans and Their Role in Shaping the Global Environment, Geophys. Monogr. Ser.*, vol. 85, edited by O. M. Johannessen, R. D. Muench, and J. E. Overland, pp. 63–76, AGU, Washington, D. C., 1994.

Fissel, D. B., J. R. Birch, H. Melling, and R. A. Lake, Non-tidal flows in the Northwest Passage, *Can. Tech. Rep. Hydrogr. Ocean Sci. 98*, Dep. of Fish. and Oceans, Inst. of Ocean Sci., Sidney, B.C., Canada, pp. 1–143, 1988.

Goldner, D. R., On the uncertainty of the mass, heat, and salt budgets of the Arctic Ocean, *J. Geophys. Res.*, *104*(C12), 29,757–29,770, 1999.

Gordeev, V. V., J. M. Martin, I. S. Sidorov, and M. V. Sidorova, A reassessment of Eurasian river input of water sediment, major elements and nutrients to the Arctic Ocean, *Am. J. Sci.*, *296*(6), 664–691, 1996.

Grotefendt, K., K. Logemann, D. Quadfasel, and S. Ronski, Is the Arctic warming?, *J. Geophys. Res.*, *103*(C12), 27,679–27,687, 1998.

Guay, C. K. H., Barium as a tracer of Arctic halocline and river waters, M.S. thesis, Oregon State Univ., Corvallis, 1997.

Guay, C. K., and K. K. Falkner, Barium as a tracer of Arctic halocline and river waters, *Deep Sea Res., Part II*, *44*, 1543–1569, 1997.

Guay, C. K., and K. K. Falkner, A survey of dissolved barium in the estuaries of major Arctic rivers and adjacent seas, *Cont. Shelf Res.*, *18*(8), 859–882, 1998.

Guay, C. K. H., K. K. Falkner, R. D. Muench, M. Mensch, M. Frank, and R. Bayer, Wind-driven transport pathways for Eurasian Arctic river discharge, *J. Geophys. Res.*, *106*(C6), 11,469–11,480, 2001.

Jones, E. P., and L. G. Anderson, On the origin of the chemical properties of the Arctic Ocean halocline, *J. Geophys. Res.*, *91*(C9), 10,759–10,767, 1986.

Jones, E. P., L. G. Anderson, and J. H. Swift, Distribution of Atlantic and Pacific waters in the upper Arctic Ocean: Implications for circulation, *Geophys. Res. Lett.*, *25*(6), 765–768, 1998.

Jones, E. P., J. H. Swift, L. G. Anderson, M. Lipizier, G. Civitarese, K. K. Falkner, G. Kattner, and F. A. McLaughlin, Tracing Pacific water in the North Atlantic Ocean, *J. Geophys. Res.*, *108*(C4), 3116, doi:10.1029/2001JC001141, 2003.

Macdonald, R. W., E. C. Carmack, F. A. McLaughlin, K. K. Falkner, and J. H. Swift, Connections among ice, runoff, and atmospheric forcing in the Beaufort Gyre, *Geophys. Res. Lett.*, *26*(15), 2223–2226, 1999.

Mackenzie-River-Basin-Committee, Mackenzie River Basin Water Quality Data 1960–1979, report, 1080 pp., Environ. Canada, Ottawa, Ont., 1981.

Mauritzen, C., Production of dense overflow waters feeding the North Atlantic across the Greenland-Scotland Ridge. part 2: An inverse model, *Deep Sea Res., Part I*, *43*, 807–835, 1996a.

Mauritzen, C., Production of dense overflow waters feeding the North Atlantic across the Greenland-Scotland Ridge. part 1: Evidence for a revised circulation scheme, *Deep Sea Res., Part I*, *43*, 796–806, 1996b.

Meredith, M., K. Heywood, P. Dennis, L. Goldson, R. White, E. Farbach, U. Schauer, and S. Østerhus, Freshwater fluxes through the western Fram Strait, *Geophys. Res. Lett.*, *28*(8), 1615–1618, 2001.

Östlund, H. G., and G. Hut, Arctic Ocean water mass balance from isotope data, *J. Geophys. Res.*, *89*(C4), 6373–6381, 1984.

Proshutinsky, A. Y., and M. A. Johnson, Two circulation regimes of the wind-driven Arctic Ocean, *J. Geophys. Res.*, *102*(C6), 12,493–12,514, 1997.

Rigor, I. G., J. M. Wallace, and R. L. Colony, On the response of the Arctic Sea ice to the Arctic oscillation, *J. Clim.*, *15*(18), 2648–2668, 2002.

Schauer, U., (Ed.), *The Expedition ARKTIS XV/3 of the Research Vessel "Polarstern" in 1999*, 63 pp., Alfred Wegener Inst. for Polar and Mar. Res., Bremerhaven, Germany, 2000.

Steele, M., and T. Boyd, Retreat of the cold halocline layer in the Arctic Ocean, *J. Geophys. Res.*, *103*(C5), 10,419–10,435, 1998.

Swift, J. H., and K. Aagaard, Seasonal transitions and water mass formation in the Iceland and Greenland Seas, *Deep Sea Res., Part A*, *28*, 1107–1129, 1981.

Swift, J. H., K. Aagaard, and S. Malmberg, The contribution of the Denmark Strait overflow to the deep North Atlantic, *Deep Sea Res., Part A*, *27*, 29–42, 1980.

Swift, J. H., E. P. Jones, K. Aagaard, E. C. Carmack, M. Hingston, R. W. Macdonald, F. A. McLaughlin, and R. G. Perkin, Waters of the Makarov and Canada basins, *Deep Sea Res., Part II*, *44*, 1503–1529, 1997.

Weeks, W. F., and S. F. Ackley, The growth, structure and properties of sea ice, in *The Geophysics of Sea Ice*, edited by N. Untersteiner, pp. 9–164, Plenum, New York, 1986.

Zhang, J., D. A. Rothrock, and M. Steele, Warming of the Arctic Ocean by a strengthened Atlantic inflow: Model results, *Geophys. Res. Lett.*, *25*(10), 1745–1748, 1998.

————————————

K. K. Falkner, College of Oceanic and Atmospheric Sciences, Oregon State University, Corvallis, OR 97331-5503, USA. (kfalkner@coas.oregonstate.edu)

M. Meredith, NERC, Proudman Oceanographic Laboratories, Bidston Observatory, Prenton, Cheshire CH43 7RA, UK. (mmm@pol.ac.uk)

J. R. Taylor, Department of Mechanical and Aerospace Engineering, University of California, San Diego, Building EBU II, 9500 Gilman Drive, La Jolla, CA 92093-0411, USA. (j2taylor@ucsd.edu)

U. Schauer, Alfred Wegener Institute for Polar and Marine Research, Building F-123, Bussestrasse 24, Bremerhaven D-27570, Germany. (uschauer@awi-bremerhaven.de)